

Effect of Substituents on the Molecular Shapes of π -Basic Macrotricyclic Receptors

Anne Lélias-Vanderperre,^[a] Emmanuel Aubert,^[b] Jean-Claude Chambron,^{*[a]} and Enrique Espinosa^{*[b]}

Keywords: Cyclophanes / Receptors / Conformation analysis / Steric hindrance / Substituent effects

Molecular recognition between receptor and substrate is optimized when these compounds show complementary shapes, sizes, and interacting moieties. A family of C_{3v} -symmetric macrotricyclics **1–4** is presented that incorporate resorcinol- and mesitylene-derived “walls” and “cap”, respectively. These compounds feature, in principle, a tetrahedral π -basic cavity. This paper reports the effect of substituents in

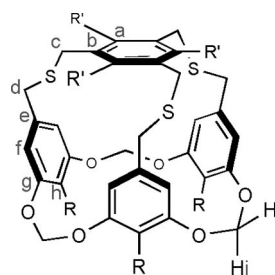
the “walls” and the “cap” on the shapes of the macrotricyclics in solution (¹H NMR), the solid state (X-ray diffraction), and gas phase (calculations). Substitution of the lower position of the “walls” by Br (in **3**) or MeS (in **4**) has the same effect as ethyl substitution of the “cap” (in **2**), that is, imparting high rigidity to the molecules and deforming their expected spherical shape to a cylindrical one.

Introduction

The specificity and selectivity of molecular recognition events between receptor and substrate are optimized when these compounds are complementary in terms of shape, size, and interacting moieties.^[1–3] These observations have ultimately led to the concept of preorganization between host and guest, which was originally illustrated by the spherands of Cram.^[4] These alkali-metal-cation receptors are rigid analogues of Pedersen’s crown ethers and Lehn’s cryptands.^[1,2] They owe this property to the fact that they are made only from aromatic subunits that are directly connected to each other. The design of receptors that are preorganized for optimum substrate recognition has been a challenge since then. For example, genuine calixarenes, which can be considered as deriving from spherands by the incorporation of methylene connectors between the aryl subunits, are flexible molecules that exist in several conformations.^[5] The problem of fixing either one has been solved by intramolecular bridging or by substituting the phenolic oxygen atoms with appropriate groups (e.g., *n*Pr).^[6]

We recently reported the synthesis and properties of macrotricyclic molecules **1** and **2**^[7] incorporating resorcinol- and mesitylene-derived “walls” and “cap”, respectively (Figure 1), and complementing molecular cages derived from hexahomotrioxacalix[3]arene.^[8] These compounds

feature π -electron-rich tetrahedral cavities and were shown (ESI-MS) to complex NH_4^+ selectively over alkali metal cations and the bulky primary ammonium *t*BuNH₃⁺ in the gas phase, presumably through cation– π interactions. This report introduces analogues of macrotricyclic **1** that carry a substituent at the C-h position of the resorcinol subunits (Br for **3**, CH₃S for **4**, Figure 1). Macrotricyclic **4** combines a cavity and a tripod thioether chelate.^[9] It was designed for the Cu^I-directed encapsulation^[10] of ethylene in order to model the biological receptor of this natural hormone in analogy with previous work involving the [9]aneS₃ macrocycle.^[11] Macrotricyclic **3** was considered a direct precursor of **4**. The synthetic aspects are first presented followed by a study of the effect of substituents on either the “cap” (Et for **2**) or the “walls” (Br and CH₃S for **3** and **4**, respectively) on the shapes of these molecules in solution (¹H NMR), in the solid state (X-ray crystallography), and in the gas phase (calculations). Finally, the implications of the structural differences are discussed with regard to the preorganization of receptors **1** and **2** for gas-phase π -complexation properties studied in a previous investigation.^[7]



- 1: R = H, R' = H
- 2: R = H, R' = Et
- 3: R = Br, R' = H
- 4: R = CH₃S, R' = H

[a] ICMUB (UMR no. 5260 of the CNRS), Université de Bourgogne, 9, avenue Alain Savary, BP 47870, 21078 Dijon, France
Fax: +33-3-80396117
E-mail: Jean-Claude.Chambron@u-bourgogne.fr

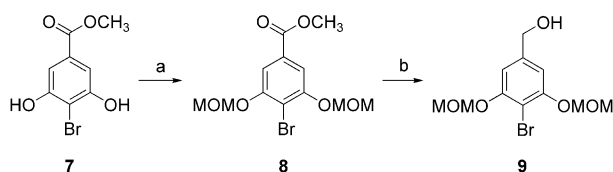
[b] CRM2 (UMR no. 7036 of the CNRS), Nancy Université, Boulevard des Aiguillettes, BP 239, 54506 Vandœuvre-lès-Nancy, France

Supporting information for this article is available on the WWW under <http://dx.doi.org/10.1002/ejoc.200901398>.

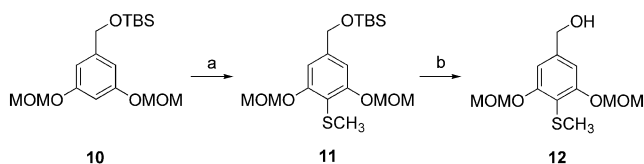
Figure 1. Chemical structures of macrotricyclics **1–4**. Atom labels are shown in grey.

Results and Discussion

The macrotricycles **1–4** used in this study were obtained by intramolecular cyclization of tripod precursors (a relatively common strategy for the synthesis of basket-shaped, C_{3v} -symmetric macrotricycles^[12]) bearing pendant resorcinol functionalities that are connected by formaldehyde acetal bridges in analogy with the formation of cavitands from resorcinarenes.^[13] The synthesis of macrotricycles **1** and **2** has been reported previously.^[7] The synthesis of the tripod precursors **5** and **6** of the macrotricycles **3** and **4**, respectively, started with functional-group transformations of the resorcinol derivatives **7** and **10** (Scheme 1 and Scheme 2). Accordingly, methyl 4-bromo-3,5-dihydroxybenzoate (**7**) was treated with MOMCl in the presence of H nig's base (*i*Pr₂NEt) to afford ester **8** in 85% yield. The latter was subsequently reduced to 4-bromobenzyl alcohol **9** by DIBAL-H in 96% yield.^[14] The corresponding 4-methylthio derivative was prepared by a different route (Scheme 2). Ortho-lithiation of **10**^[15] by *n*BuLi in the presence of TMEDA followed by quenching with elemental sulfur and in situ reaction of the resulting thiophenolate with CH₃I afforded methyl thioether **11** in 66% yield. The TBS protection was cleaved by reaction of **11** with TBAF and 4-methylthiobenzyl alcohol **12** was obtained in 99% yield. The benzyl thiol analogues **15** and **16** of the benzyl alcohols **9** and **12**, respectively, were prepared in two steps from the latter compounds (Scheme 3). First, **9** (resp. **12**) was treated with AcSH under Mitsunobu conditions (DIAD, PPh₃, 0  C) to produce thioacetate derivatives **13** (resp. **14**) in 49% (resp. 70%) yield. Methanolysis (K₂CO₃, CH₃OH) of **13** and reduction (LiAlH₄) of **14** followed by quenching of the reaction mixture with dilute aqueous HCl afforded benzyl thiols **15** (92%) and **16** (96%), respectively.

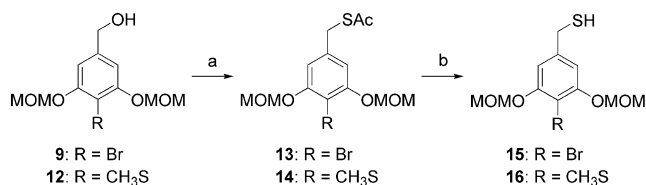


Scheme 1. Synthesis of benzyl alcohol **9**. Reagents and conditions: a) MOMCl, *i*PrNEt, THF, 85%; b) DIBAL-H, THF/CH₂Cl₂, 96%.



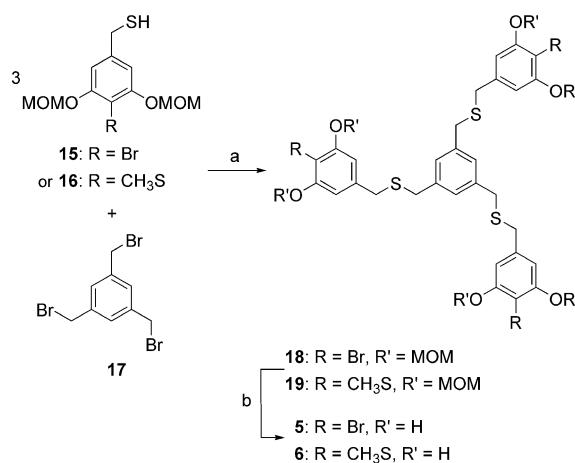
Scheme 2. Synthesis of benzyl alcohol **12**. Reagents and conditions: a) i. *n*BuLi, TMEDA; ii. S₈; iii. CH₃I, 66%; b) (*n*Bu₄N)F, THF, 99%.

Tripods **5** and **6** were synthesized in two steps from benzyl thiols **15** and **16**, respectively (Scheme 4). Deprotonation of **15** and **16** with NaH followed by a triple condensation reaction with 1,3,5-tris(bromomethyl)benzene (**17**) afforded the MOM-protected tripods **18** and **19** in 79 and 100% yields, respectively. Standard conditions for cleavage of the



Scheme 3. Syntheses of benzyl thiols **15** and **16**. Reagents and conditions: a) AcSH, DIAD, PPh₃, 49% for **13**, 70% for **14**; b) K₂CO₃/CH₃OH, 92% for **15**; LiAlH₄/THF, 96% for **16**.

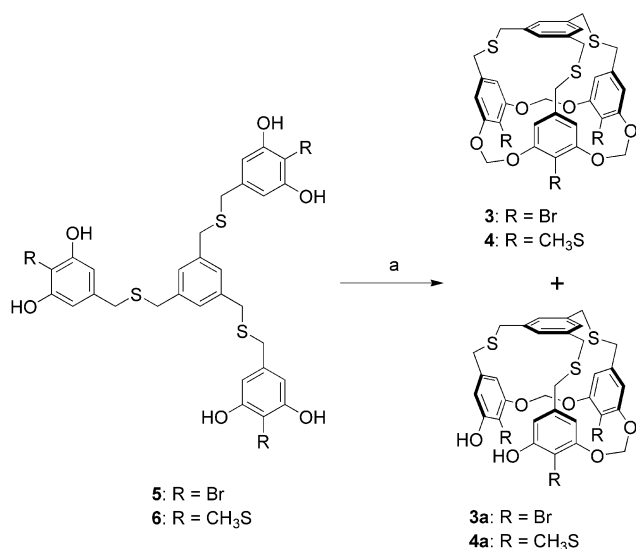
MOM protecting groups (aqueous HCl) induces cleavage of the benzylic thioether bridges and thus non-hydrolytic conditions were examined.^[16] Accordingly, tripods **18**, **19** were treated with *p*-toluenesulfonic acid in CH₂Cl₂/CH₃OH, which produced the target tripods **5**, **6** in 87 and 100% yield, respectively.



Scheme 4. Preparation of tripods **5** and **6**. Reagents and conditions: a) NaH, THF, 79% for **18**, 100% for **19**; b) *p*TsOH, CH₂Cl₂/CH₃OH, 87% for **5**, 100% for **6**.

Macrotricycles **3** and **4** were prepared by three-fold ring-closure condensation reaction of tripods **5** and **6**, respectively, with dibromomethane in the presence of Cs₂CO₃ as base in high dilution conditions (9×10^{-4} M in DMF at 60  C), as shown in Scheme 5. They were obtained in 4.8 and 6% yields, respectively, which is very much lower than the 18% yield of **1** obtained under the same reaction conditions.^[7] This indicates that the cyclization reactions are hampered by the presence of the bulky Br (for **3**) and CH₃S (for **4**) substituents. In support of this assertion, the intermediate macrobicyclic product of two-fold ring closure (**4a**) was isolated in trace amounts in the course of the chromatographic purification of macrotricyclic **4**. As a result of the poor yields obtained from the macrotricyclization reactions, the direct preparation of **4** from **3** was not attempted.

The first evidence that the polycyclic structures **3**, **4a**, and **4** had indeed been formed was provided by electrospray mass spectrometry. In all three cases the signal corresponding to the sodium adduct of the species investigated was observed and the corresponding isotope peak cluster was in agreement with the calculated one (Figures S15–S17 of the



Scheme 5. Preparation of macrotricycles **3** and **4**. Reagents and conditions: a) CH₂Br₂, Cs₂CO₃, DMF, 60 °C, 4.8% for **3**, 6% for **4**. In the case of the latter, the intermediate macrobicyclic **4a** was isolated in minor amounts by chromatography.

Supporting Information). That the sodium rather than the proton adduct was observed is not surprising in the light of previous studies involving macrotricycles **1** and **2**.

An ORTEP view of the X-ray crystal structure of macrotricyclic **1** is shown in Figure 2 together with the already known one of macrotricyclic **2**.^[7] Unlike **2**, which shows a well-defined but elongated (cylindrical) cavity in the solid state, **1** has a collapsed structure because the mesitylene “cap” has a weak interaction (ring-to-ring distance of 3.981 Å) with one of the resorcinol-derived aromatic “walls”.

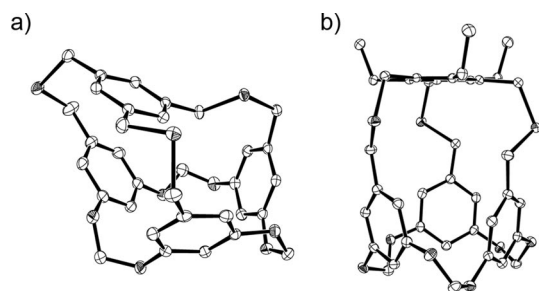


Figure 2. Comparison of the X-ray crystal structures of macrotricycles (a) **1** and (b) **2**.^[7] Hydrogen atoms have been omitted for clarity. Thermal ellipsoids are drawn at the 50% probability level.

Gas-phase DFT calculations were performed at the PBE1PBE 6-311G** level of theory using the X-ray molecular structures of **1** and **2** as the starting points. All four compounds **1–4** showed stable collapsed and elongated conformations (Figures S19–S22 and Figure 3) with large energy differences between them (Table 1). Macrotricyclic **1** is more stable in the collapsed conformation, which is in agreement with the experimental solid-state structure. In contrast, macrotricycles **2–4** are significantly more stable in the elongated form, as is also observed in the solid state for

2. The largest energy differences are obtained for compounds **3** and **4** in spite of short S...S (3.47 and 3.38 Å, respectively) and Br...Br (3.55 and 3.54 Å, respectively) interatomic contacts in the collapsed form (Figures S21 and S22). As shown in Figure 3, the most stable optimized structures (elongated forms) of macrotricycles **3** and **4** are very similar to that of **2** even though their substituents are in positions that differ from those of the latter macrotricyclic.

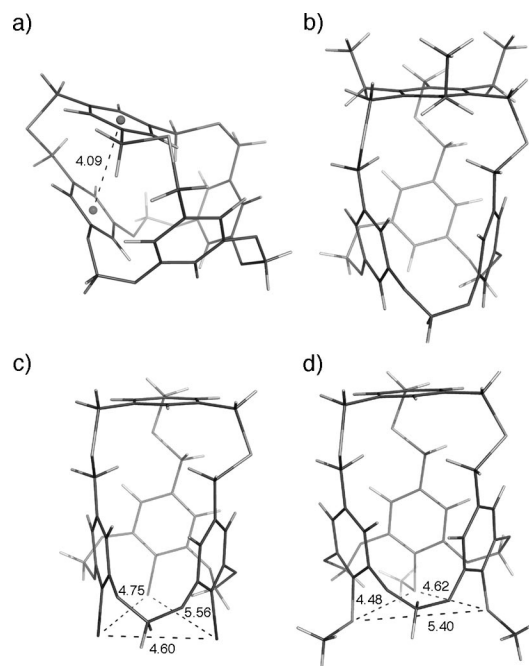


Figure 3. Representation (sticks) of the molecular structures optimized at the DFT PBE1PBE 6-311G** level of theory (distances between centroids or heteroatoms in Å) for the macrotricycles a) **1**, b) **2**, c) **3**, and d) **4**.

Table 1. Gas-phase calculated standard free energy differences ($\Delta G^0 = \Delta G^0_{\text{elong.}} - \Delta G^0_{\text{coll.}}$) between the elongated and collapsed forms of macrotricycles **1–4**.

Macrotricyclic	1	2	3	4
ΔG^0 [kJ mol ⁻¹]	20.09	-33.44	-51.93	-56.41

The solution structures of macrotricycles **1–4** were elucidated by ¹H NMR spectroscopy. The spectra were fully assigned through 2D ¹H/¹³C HSQC and HMBC, and ¹H/¹H NOESY experiments (Figures S1–S7 of the Supporting Information). The chemical shifts of the protons relevant to this study are collected in Table 2. Careful examination of the data shows that the protons of macrotricycles **3** and **4** and, to a lesser extent, of macrotricyclic **2** have similar chemical shifts, which suggests that the conformations of these molecules are similar and are controlled by the bulky substituent on the C-h atoms, that is, Br (for **3**) and CH₃S (for **4**), or the ethyl substitution of C-a for **2**. In contrast, the ¹H NMR spectrum of macrotricyclic **1**, which lacks any substituent at these positions, is significantly different to those of **2–4**, the most striking features being the relatively

high-field shift of the signal of proton a-H in the former, and the inversion of the relative values of the chemical shifts of protons c-H and d-H (Table 2).

Table 2. ¹H NMR chemical shifts for macrotricycles 1–4.

Compd.	δ [ppm]						
	a	c	d	f	h	i	j
1 ^[a,b]	6.47	3.24	3.69	6.50	6.80	5.60	5.72
2 ^[a,b]	–	3.86	3.25	6.40	6.33	5.50	5.65
3 ^[c]	7.11	3.78	3.15	6.54	–	5.53	6.07
4 ^[b]	7.13	3.80	3.11	6.60	–	5.48	5.97

[a] Data from ref.^[7]. [b] Determined in CDCl₃. [c] Determined in CD₂Cl₂.

Examination of these data and of the NOE correlations observed in compounds 1–4 (Figure 4) shows that the mesitylene “cap” has a different conformation in 1 in comparison with 2–4. In the case of the unsubstituted macrotricycle 1 it is squeezed by twisting towards the cage inside, hence the shielding of the a-H and c-H protons by the resorcinol “walls” and the NOE correlation c-H/f-H, which is absent in the spectra of the macrotricycles 2–4. In the case of the macrotricycles 3 and 4, a-H has a quasi-normal δ value for an aromatic proton, whereas d-H is shielded relative to c-H and a NOE correlation between a-H and d-H is observed. This suggests that the mesitylene “cap” is fully untwisted, which places d-H in its shielding field. This conformational difference is a result of the steric repulsion between the large substituents of C-h, Br in the case of 3, CH₃S in the case of 4. Therefore steric interactions at the lower part of macrotricycles 3 and 4 are mechanically conveyed to the upper part of the molecules and translated into an untwisting of the mesitylene “cap”. Macrotricycle 2 shows similar features to 3 and 4 (i.e., shielding of d-H, deshielding of c-H, and an Et-H/d-H NOE correlation, which parallels the a-H/d-H correlation seen in the latter compounds). These observations indicate that the mesitylene “cap” is also untwisted in 2. In 2 this conformational feature is not due to remote steric effects, but to the presence of the ethyl substituents. This is clearly apparent from the X-ray crystal structure (Figure 2, b), which also shows that, as a consequence of the stiffening of its upper part,

the molecule has a cylindrical rather than a spherical shape. On the basis of the ¹H NMR spectroscopic data, it is likely that macrotricycles 3 and 4 adopt similar structures.

Another stereochemical feature of the macrotricycles in solution is the conformation of the formaldehyde acetal bridges. Careful examination of Figure 3 shows three types of orientations for protons i-H and j-H in the gas phase: Axial-up j-H and equatorial i-H, axial-down i-H and equatorial j-H (Figure 3, a), and both i-H and j-H pointing down towards the inside (inside-down) and the outside (outside-down) of the macrotricycle, respectively (Figure 3, b–d). The latter could explain the relative shielding of i-H in comparison with j-H. All four macrotricycles show a correlation between j-H and f-H in the ¹H/¹H NOESY NMR spectra, which results from axial-up j-H. In addition, the spectra of 1 and 2 show a correlation between i-H and h-H due to axial-down or inside-down i-H, which of course is lacking in the case of 3. In the case of 4, the correlation i-H/CH₃S is observed, which is presumably due to equatorial i-H, as outside-down j-H and inside-down i-H should both interact with CH₃S. Protons i-H and j-H form a diastereotopic pair at room temperature. Variable-temperature ¹H NMR experiments on macrotricycles 1 and 3 up to 408 K in C₂D₂Cl₄ did not show any coalescence phenomena, which indicates that the macrotricycles do not invert on the NMR timescale (Figures S11 and S12 of the Supporting Information). In addition, most of the protons, in particular a-H and c-H of the mesitylene “cap” of 1, show downfield shifts upon increasing the temperature from 298 to 408 K (Table 3).

Table 3. Variations in the ¹H NMR chemical shifts of macrotricycles 1 and 3 upon temperature increase between 298 and 408 K^[a] and between 182 and 300 K.^[b]

Compd.	$\Delta\delta$ [ppm]						
	a	c	d	f	h	i	j
1 ^[a]	0.14	0.14	0.02	0.01	0.06	0.06	0.01
1 ^[b]	0.22	0.21	0.02	0.08	0.02	0.04	0.02
3 ^[a]	0.06	0.06	0.07	0.06	–	0.08	–0.01
3 ^[b]	0.06	0.06	0.03	0.12	–	–0.03	–0.07

[a] Determined in C₂D₂Cl₄ (298–408 K). [b] Determined in CD₂Cl₂ (182–300 K).

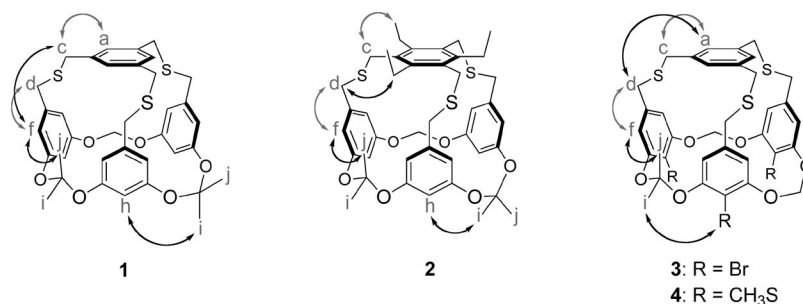


Figure 4. NOE correlations observed in macrotricycles 1–4. Those conveying structural information are highlighted in black. The different orientations adopted by protons i-H and j-H (from DFT optimizations, see Figure 3) are also shown. The arrow connecting i-H and R concerns macrotricycle 4 (R = CH₃S).

Cooling CD_2Cl_2 solutions of macrotricyclic **1** from 300 to 182 K produces broadening of the signals and a significant upfield shift of a-H by -0.22 ppm and c-H by -0.21 ppm at 182 K (Figures S13 and S14 of the Supporting Information). This indicates again that the dynamics of the mesitylene “cap” are affected more than other parts of the molecule by temperature changes. In short, motion within the macrocycle is only slowed by decreasing the temperature. In the case of **3**, the signals are lower in intensity and broaden strongly, and, as in the high-temperature regime when the temperature is decreased, they undergo small upfield shifts. Maximum broadening is observed at 200 K at which coalescence takes place; below this temperature there are two sets of signals, one corresponding to a major species and the other corresponding to a very minor species. The major subspectrum is very similar to the room-temperature spectrum, which indicates that the corresponding species has a conformation that is very close to that of the starting system (virtually no temperature-induced shifts). The minor subspectrum, which corresponds to a highly unsymmetrical conformation, is very different. Upon decreasing the temperature further, the signals sharpen again, which confirms the occurrence of dynamic phenomena.

Conclusions

This study has shown that the experimental structures of macrotricyclics **1** and **2** are very different in the solid state as well as in solution. These observations have been confirmed by theoretical calculations at the PBE1PBE 6-311G** level of theory. Macrotricyclic **1**, being highly flexible, has an average spherical tetrahedral shape, whereas macrotricyclic **2**, being stiffened by persubstitution of the mesitylene “cap”, takes up an elongated tetrahedral shape.^[17] In addition, as shown by ^1H NMR studies, substitution of the 2-position (C-h) of the resorcinol-derived subunits by relatively large heteroatom-bearing groups (Br in **3**, CH_3S in **4**) has the same effect as persubstitution of the mesitylene “cap”. Interestingly, in spite of important structural differences, macrotricyclics **1** and **2** both show selective affinity for NH_4^+ over K^+ in the gas phase (ESI-MS).^[7] This suggests either that NH_4^+ forms $\text{NH}^+\cdots\pi$ interactions only with the more electron-rich resorcinol-derived aromatic walls or that the energy of interaction of NH_4^+ with macrotricyclic **2** is large enough to change the structure of the latter to a spherical conformation.

Experimental Section

General: Macrotricyclics **1** and **2** were obtained from a previous study.^[7] 3,5-Bis(methoxymethoxy)benzyl *tert*-butyldimethylsilyl ether (**10**)^[15] and 1,3,5-tris(bromomethyl)benzene (**17**)^[18] were synthesized according to procedures reported in the literature. All reactions were performed under dinitrogen using standard Schlenk techniques unless otherwise stated. THF, CH_2Cl_2 , and TMEDA were distilled from Na/benzophenone, CaH_2 , and Na, respectively. DMF was purified by filtration through standardized aluminium oxide 90. They were stored under dinitrogen over 4 Å molecular

sieves before use. All commercially available products were reagent grade and used without further purification. Flash column chromatography was performed by using 35–70 mesh silica gel. NMR spectra were recorded with Bruker Avance 300, 500, and 600 spectrometers with tetramethylsilane as the internal standard. Melting points were determined with a Büchi Melting Point B-545 apparatus. Elemental analyses were performed with an EA1108 CHNS Fisons Instrument. ESI-TOF mass spectra were recorded with a Bruker Micro TOF mass spectrometer.

Methyl 4-Bromo-3,5-bis(methoxymethoxy)benzoate (8): MOMCl (3.9 mL, 50.8 mmol) was slowly added to a solution of **7** (13.2 g, 76.2 mmol) and *i*Pr₂NEt (10.9 mL, 61.0 mmol) in THF (100 mL) at 0 °C and the reaction mixture was stirred at room temperature. An additional portion of MOMCl (0.8 mL, 10.2 mmol) was added after 5.5 h. After stirring for 20 h at room temperature and then at reflux, the reaction mixture was poured into water (50 mL). The aqueous layer was extracted twice with CH_2Cl_2 . The organic layer was then washed twice with water, then 1% aqueous HCl, and finally brine. It was dried with MgSO_4 and concentrated. The crude product was crystallized from hot EtOAc to afford yellow needles of **8** (5.81 g, 85% yield), m.p. 138.5–141.7 °C. ^1H NMR (500 MHz, CDCl_3 , 25 °C): δ = 3.53 (s, 6 H, CH_3O), 3.89 (s, 3 H, CH_3O), 5.29 (s, 4 H, CH_2O), 7.48 (s, 2 H, CH) ppm. ^{13}C NMR (75 MHz, CDCl_3 , 25 °C): δ = 52.6 (CH_3O), 56.7 (CH_3OCH_2), 95.2 (CH_2O), 109.5 (CBr), 110.1 (CH), 130.5 (CO), 154.9 (C=O), 166.3 (C=O) ppm. $\text{C}_{12}\text{H}_{15}\text{O}_6\text{Br}$ (335.15): calcd. C 43.00, H 4.51; found C 42.79, H 4.83.

[4-Bromo-3,5-bis(methoxymethoxy)phenyl]methanol (9): DIBAL-H (22.4 mL, 22.4 mmol, 1 M in hexane) was added dropwise to a solution of **8** (3.00 g, 8.95 mmol) in THF (30 mL) and CH_2Cl_2 (50 mL) at 0 °C. After stirring for 2 h at room temperature, water (10 mL) and then 10% aqueous NaOH (5 mL) were slowly added at 0 °C. The precipitate was removed by filtration and washed with CH_2Cl_2 and EtOAc. The solution was concentrated to afford **9** as a colorless solid (2.65 g, 96% yield), m.p. 57.4 °C. ^1H NMR (500 MHz, CDCl_3 , 25 °C): δ = 3.51 (s, 6 H, CH_3O), 4.64 (s, 2 H, CH_2OH), 5.26 (s, 4 H, CH_2O), 6.85 (s, 2 H, CH) ppm. ^{13}C NMR (75 MHz, CDCl_3 , 25 °C): δ = 56.6 (CH_3O), 65.0 (CH_2OH), 95.2 (CH_2O), 102.7 (CBr), 107.8 (CH), 141.9 (CCH_2), 155.1 (CO) ppm. $\text{C}_{11}\text{H}_{15}\text{O}_5\text{Br}$ (307.14): calcd. C 43.02, H 4.92; found C 42.96, H 5.28.

3,5-Bis(methoxymethoxy)-4-methylthiobenzyl *tert*-Butyldimethylsilyl Ether (11): A solution of *n*-BuLi (4.4 mL, 11.1 mmol, 2.5 M in hexane) was added to a mixture of **10** (2.71 g, 7.9 mmol) and TMEDA (7.7 mL, 11.1 mmol) in THF (50 mL) at -40 °C. After stirring for 9 h, sulfur (0.31 g, 9.5 mmol) followed by MeI (0.6 mL, 9.5 mmol) were added to the reaction mixture. Stirring was continued overnight at room temperature. Subsequent addition of water (40 mL) was followed by extraction of the aqueous layer with CH_2Cl_2 (twice). The organic layer was then washed twice with water and brine, dried with MgSO_4 , and concentrated. The residue was purified by flash column chromatography (SiO_2 , $\text{CH}_2\text{Cl}_2/n$ -heptane, 90:10 to 98:2) to afford **11** as a colorless oil (2.02 g, 66% yield). ^1H NMR (300 MHz, CDCl_3 , 25 °C): δ = 0.09 (s, 6 H, SiCH_3), 0.94 (s, 9 H, CCH_3), 3.51 (s, 6 H, CH_3O), 4.67 (s, 3 H, CH_3S), 4.67 (s, 2 H, CH_2OSi), 5.24 (s, 4 H, CH_2O), 6.84 (s, 2 H, CH) ppm. ^{13}C NMR (75 MHz, CDCl_3 , 25 °C): δ = -5.2 (CH_3Si), 18.3 (CH_3S), 18.5 (CCH_3), 26.0 (CCH_3), 56.4 (CH_3O), 64.7 (CH_2OSi), 95.2 (CH_2O), 106.7 (CH), 113.1 (CS), 143.8 (CCH_2), 158.5 (CO) ppm. ^{29}Si NMR (99 MHz, CDCl_3 , 25 °C): δ = 21.20 ppm. $\text{C}_{18}\text{H}_{32}\text{O}_5\text{SSi}$ (388.60): calcd. C 55.64, H 8.30; found C 55.43, H 8.42.

[3,5-Bis(methoxymethoxy)-4-methylthiophenyl]methanol (12): TBAF (9.02 mL, 9.02 mmol, 1 M in THF) was added to a solution of **11** (1.75 g, 4.51 mmol) in THF (20 mL) at 0 °C and the reaction mixture was stirred for 5 h. It was subsequently quenched by addition of a saturated solution of aqueous NH₄Cl (9 mL). The aqueous layer was extracted with ethyl acetate. The organic layer was washed twice with water and brine, dried with MgSO₄, and concentrated. The residue was purified by flash column chromatography (SiO₂, CH₂Cl₂/CH₃OH, 96:4) to give **12** as a colorless oil (1.23 g, 99% yield). ¹H NMR (300 MHz, CDCl₃, 25 °C): δ = 2.39 (s, 3 H, CH₃S), 3.52 (s, 6 H, CH₃O), 4.65 (s, 2 H, CH₂OH), 5.27 (s, 4 H, CH₂O), 6.86 (s, 2 H, CH) ppm. ¹³C NMR (75 MHz, CDCl₃, 25 °C): δ = 18.2 (CH₃S), 56.5 (CH₃O), 65.2 (CH₂OH), 95.2 (CH₂O), 107.4 (CH), 114.1 (CS), 142.9 (CCH₂), 158.7 (CO) ppm. C₁₂H₁₈O₅S (274.33): calcd. C 52.53, H 6.61; found C 52.76, H 6.98.

4-Bromo-3,5-bis(methoxymethoxy)benzyl Thioacetate (13): A mixture of thioacetic acid (0.95 mL, 13.02 mmol) and **9** (2.0 g, 6.51 mmol) in THF (20 mL) was added slowly to a mixture of DIAD (1.72 mL, 8.14 mmol) and triphenylphosphane (2.16 g, 8.14 mmol) in THF (30 mL) at 0 °C. After stirring overnight at room temperature, the solvent was removed in vacuo. The residue was purified by repeated column chromatography on silica eluting with EtOAc/*n*-heptane (88:12) to afford **13** as a colorless oil (1.17 g, 49% yield). ¹H NMR (500 MHz, CDCl₃, 25 °C): δ = 2.35 (s, 3 H, COCH₃), 3.52 (s, 6 H, CH₃O), 4.04 (s, 2 H, CH₂S), 5.22 (s, 4 H, CH₂O), 6.77 (s, 2 H, CH) ppm. ¹³C NMR (75 MHz, CDCl₃, 25 °C): δ = 30.5 (CH₃C=O), 33.7 (CH₂S), 56.7 (CH₃O), 95.3 (CH₂O), 102.8 (CBr), 110.2 (CH), 138.5 (CCH₂), 155.0 (CO), 195.0 (C=O) ppm. C₁₃H₁₇O₅BrS (365.25): calcd. C 42.75, H 4.69, S 8.78; found C 42.92, H 4.82, S 8.69.

3,5-Bis(methoxymethoxy)-4-methylthiobenzyl Thioacetate (14): Synthesized following the procedure used for **13** from **12** (1.15 g, 4.17 mmol), thioacetic acid (0.61 mL, 8.35 mmol), DIAD (1.01 mL, 3.05 mmol), and triphenylphosphane (1.27 g, 4.80 mmol) in THF (40 mL). Thioacetate **14** was obtained in 70% yield (0.97 g) as a yellow oil after purification by flash column chromatography (SiO₂, CH₂Cl₂/*n*-heptane, 90:10 followed by *n*-heptane/ethyl acetate, 75:25). ¹H NMR (300 MHz, CDCl₃, 25 °C): δ = 2.35 (s, 3 H, COCH₃), 2.37 (s, 3 H, CH₃S), 3.52 (s, 6 H, CH₃O), 4.06 (s, 2 H, CH₂S), 5.24 (s, 4 H, CH₂O), 6.77 (s, 2 H, CH) ppm. ¹³C NMR (75 MHz, CDCl₃, 25 °C): δ = 18.1 (CH₃S), 30.5 (CH₃C=O), 33.8 (CH₂S), 56.6 (CH₃O), 95.3 (CH₂O), 109.7 (CH), 114.2 (CS), 139.3 (CCH₂), 158.6 (CO), 195.0 (C=O) ppm. C₁₄H₂₀O₅S₂ (332.44): calcd. C 50.58, H 6.06, S 19.29; found C 50.61, H 6.18, S 19.92.

[4-Bromo-3,5-bis(methoxymethoxy)phenyl]methanethiol (15): K₂CO₃ (1.33 g, 9.64 mmol) was added portionwise to a solution of **13** (1.17 g, 3.21 mmol) in methanol (15 mL). After stirring overnight at room temperature, 1% aqueous HCl (70 mL, 19.3 mmol) was added dropwise at 0 °C. The aqueous layer was extracted twice with ethyl acetate and CH₂Cl₂. The organic layer was washed twice with brine, dried with MgSO₄, and concentrated to give **15** as an oil (0.96 g, 92% yield). ¹H NMR (500 MHz, CDCl₃, 25 °C): δ = 1.79 (t, ³J_{H,H} = 8 Hz, 1 H, SH), 3.52 (s, 6 H, CH₃O), 3.67 (d, ³J_{H,H} = 8 Hz, 2 H, CH₂S), 5.25 (s, 4 H, CH₂O), 6.82 (s, 2 H, CH) ppm. ¹³C NMR (75 MHz, CDCl₃, 25 °C): δ = 29.2 (CH₂S), 56.6 (CH₃O), 95.3 (CH₂O), 102.6 (CBr), 109.4 (CH), 142.1 (CCH₂), 155.1 (CO) ppm. C₁₁H₁₅O₄BrS·0.25C₄H₈O₂ (345.23): calcd. C 41.75, H 4.96, S 9.29; found C 42.08, H 4.84, S 9.64.

[4-Methylthio-3,5-bis(methoxymethoxy)phenyl]methanethiol (16): A solution of **14** (0.97 g, 2.91 mmol) in THF (20 mL) was added dropwise to a suspension of LiAlH₄ (0.23 g, 5.82 mmol) in THF (40 mL) at 0 °C. The reaction mixture was stirred for 5 h at reflux.

Then 5% aqueous HCl (4.3 mL) was carefully added to the reaction mixture at 0 °C. The aqueous layer was extracted twice with ethyl acetate and CH₂Cl₂. The organic layer was then washed twice with water and brine, dried with MgSO₄, concentrated, and dried to afford **16** as an oil (0.81 g, 96% yield). ¹H NMR (300 MHz, CDCl₃, 25 °C): δ = 1.80 (t, ³J_{H,H} = 7.8 Hz, 1 H, SH), 2.39 (s, 3 H, CH₃S), 3.53 (s, 6 H, CH₃O), 3.68 (d, ³J_{H,H} = 7.8 Hz, 2 H, CH₂S), 5.27 (s, 4 H, CH₂O), 6.82 (s, 2 H, CH) ppm. ¹³C NMR (75 MHz, CDCl₃, 25 °C): δ = 18.2 (CH₃S), 29.4 (CH₂S), 56.6 (CH₃O), 95.2 (CH₂O), 108.9 (CH), 113.8 (CS), 143.0 (CCH₂), 158.6 (CO) ppm. C₁₂H₁₈O₄S₂·0.25C₄H₈O₂ (312.43): calcd. C 49.97, H 6.45, S 20.53; found C 50.24, H 6.41, S 21.16.

Tripod 18: A solution of **17** (0.29 g, 0.82 mmol) in THF (15 mL) was added portionwise to a mixture of NaH (60% in oil, 0.10 g, 2.55 mmol) and **15** (0.82 g, 2.54 mmol) in THF (20 mL) at 0 °C. The reaction mixture was stirred for 2 h at room temperature. A saturated aqueous solution of NH₄Cl was added at 0 °C until pH 6. The aqueous layer was extracted with EtOAc. The organic layer was washed twice with brine, dried with MgSO₄, and concentrated. The residue was purified by column chromatography (SiO₂, *n*-heptane/EtOAc, 68:32) to give **18** as a colorless oil (0.70 g, 79% yield). ¹H NMR (500 MHz, [D₆]acetone): δ = 3.43 (s, 18 H, CH₃), 3.56 (s, 6 H, d-H), 3.63 (s, 6 H, c-H), 5.23 (s, 12 H, CH₂O), 6.82 (s, 6 H, f-H), 7.13 (s, 3 H, a-H) ppm. ¹³C NMR (75 MHz, [D₆]acetone): δ = 35.8 (C-c), 36.1 (C-d), 56.6 (CH₃O), 95.8 (CH₂O), 102.3 (C-h), 110.7 (C-f), 129.3 (C-a), 139.8 (C-b), 140.5 (C-e), 155.7 (C-g) ppm. C₄₂H₅₁O₁₂Br₃S₃ (1083.75): calcd. C 46.55, H 4.74, S 8.87; found C 46.26, H 4.99, S 8.88.

Tripod 19: Synthesized following the procedure used for **18** from **16** (0.61 g, 2.10 mmol), NaH (60% in oil, 85 mg, 2.13 mmol), and **17** (0.25 g, 0.69 mmol) in THF (50 mL). Tripod **19** was obtained in 100% yield (0.77 g) as colorless needles after purification by crystallization from CH₂Cl₂/Et₂O (6:4), m.p. 62.2–64.2 °C. ¹H NMR (300 MHz, CD₂Cl₂, 25 °C): δ = 2.35 (s, 9 H, CH₃S), 3.48 (s, 18 H, CH₃O), 3.53 (s, 6 H, d-H), 3.61 (s, 6 H, c-H), 5.21 (s, 12 H, CH₂O), 6.75 (s, 6 H, f-H), 7.14 (s, 3 H, a-H) ppm. ¹³C NMR (75 MHz, CD₂Cl₂, 25 °C): δ = 18.1 (CH₃S), 35.9 (C-c), 36.2 (C-d), 56.6 (CH₃O), 95.5 (CH₂O), 110.0 (C-f), 114.3 (C-h), 128.8 (C-a), 139.2 (C-b), 140.3 (C-e), 158.7 (C-g) ppm. C₄₅H₆₀O₁₂S₆ (985.36): calcd. C 54.85, H 6.14, S 19.53; found C 55.17, H 6.39, S 19.68.

Tripod 5: A mixture of 4-toluenesulfonic acid (3.03 g, 15.04 mmol) and **18** (0.68 g, 0.63 mmol) in MeOH (15 mL) and CH₂Cl₂ (15 mL) was stirred overnight at 25 °C. An aqueous solution of NaHCO₃ was added subsequently until pH 6. The aqueous layer was extracted twice with EtOAc. The organic layer was then washed twice with brine, dried with MgSO₄, and concentrated to give **5** as a foam (0.45 g, 87% yield). ¹H NMR (500 MHz, [D₆]acetone): δ = 3.52 (s, 6 H, d-H), 3.61 (s, 6 H, c-H), 6.53 (s, 6 H, f-H), 7.11 (s, 3 H, a-H), 8.56 (br. s, 6 H, OH) ppm. ¹³C NMR (75 MHz, [D₆]acetone): δ = 36.0 (C-c), 36.1 (C-d), 103.7 (C-h), 108.8 (C-f), 129.1 (C-a), 139.7 (C-b), 140.1 (C-e), 155.9 (C-g) ppm. C₃₀H₂₇O₆Br₃S₃·C₄H₈O₂ (781.53): calcd. C 45.00, H 3.89, S 10.60; found C 45.54, H 4.14, S 10.89.

Tripod 6: Synthesized following the procedure used for **5** from **19** (0.18 g, 0.18 mmol) and 4-toluenesulfonic acid (0.84 g, 4.39 mmol). Tripod **6** was obtained as a foam (0.15 g, 100% yield), m.p. 37 °C. ¹H NMR (300 MHz, [D₆]acetone): δ = 2.23 (s, 9 H, CH₃S), 3.54 (s, 6 H, d-H), 3.67 (s, 6 H, c-H), 6.48 (s, 6 H, f-H), 7.14 (s, 3 H, a-H), 7.99 (br. s, 6 H, OH) ppm. ¹³C NMR (75 MHz, [D₆]acetone): δ = 18.1 (CH₃S), 36.2 (C-c), 36.3 (C-d), 106.7 (C-h), 108.0 (C-f), 129.1 (C-a), 139.7 (C-b), 142.6 (C-e), 159.5 (C-g) ppm.

$C_{33}H_{36}O_6S_6 \cdot H_2O$ (739.05): calcd. C 53.63, H 5.18; found C 53.59, H 5.40.

Macrotricyclic 3: A solution of **5** (0.100 g, 0.122 mmol) and CH_2Br_2 (270 μ L, 4.03 mmol) in DMF (50 mL) was added over 7.5 h to a suspension of Cs_2CO_3 (0.26 g, 0.81 mmol) in DMF (150 mL) at 60 °C. After stirring overnight, the reaction mixture was concentrated under reduced pressure. The residue was taken up into CH_2Cl_2 and water. The aqueous layer was extracted with CH_2Cl_2 . The organic layer was then washed three times with water, dried with $MgSO_4$, and concentrated. The residue was purified by flash column chromatography (Al_2O_3 , CH_2Cl_2/n -heptane, 7:3 to 9:1, then SiO_2 , n -heptane/EtOAc, 4:6) to afford **3** as a colorless powder (5 mg, 4.8% yield). 1H NMR (300 MHz, CD_2Cl_2 , 25 °C): δ = 3.15 (s, 6 H, d-H), 3.78 (s, 6 H, c-H), 5.53 (d, $^2J_{H,H}$ = 7.7 Hz, 3 H, i-H), 6.07 (d, $^2J_{H,H}$ = 7.7 Hz, 3 H, j-H), 6.54 (s, 6 H, f-H), 7.11 (s, 3 H, a-H) ppm. ^{13}C NMR (151 MHz, CD_2Cl_2 , 25 °C): δ = 33.9 (C-d), 36.1 (C-c), 92.9 (CH_2O), 105.8 (C-h), 112.7 (C-f), 129.5 (C-a), 136.7 (C-e), 138.4 (C-b), 154.7 (C-g) ppm. HRMS: calcd. for $C_{33}H_{27}Br_3NaO_6S_3$ 874.84121; found 874.84550.

Macrotricyclic 4 and Macrobicyclic 4a: A mixture of **6** (0.14 g, 0.19 mmol) and CH_2Br_2 (45.5 μ L, 0.64 mmol) in DMF (50 mL) was added over a period of 9 h to a suspension of Cs_2CO_3 (0.76 g, 2.33 mmol) in DMF (150 mL) at 60 °C. After stirring for 3 d at 60 °C, the solvent was removed under reduced pressure. The crude product was taken up in CH_2Cl_2 and EtOAc and then filtered through Celite. The Celite cake was washed with CH_2Cl_2 . The filtrate was concentrated and purified by flash column chromatography (SiO_2 , CH_2Cl_2) to afford **4** as a colorless powder (8 mg, 6% yield). 1H NMR (300 MHz, $CDCl_3$, 25 °C): δ = 2.27 (s, 9 H, CH_3S), 3.11 (s, 6 H, d-H), 3.80 (s, 6 H, c-H), 5.48 (d, $^2J_{H,H}$ = 7.8 Hz, 3 H, i-H), 5.97 (d, $^2J_{H,H}$ = 7.8 Hz, 3 H, j-H), 6.60 (s, 6 H, f-H), 7.13 (s, 3 H, a-H) ppm. ^{13}C NMR (151 MHz, $CDCl_3$, 25 °C): δ = 18.5 (CH_3S), 34.5 (C-d), 36.4 (C-c), 96.5 (CH_2O), 115.7 (C-f), 118.0 (C-h), 129.7 (C-a), 137.1 (C-e), 138.5 (C-b), 159.2 (C-g) ppm. HRMS: calcd. for $C_{36}H_{36}NaO_6S_6$ 779.07383; found 779.07588.

4a: 1H NMR (500 MHz, $CDCl_3$, 25 °C): δ = 2.06 (s, 3 H, CH_3S''), 2.34 (s, 6 H, CH_3S), 3.40 (AB, J_{AB} = 14.0, $\Delta\nu$ = 90 Hz, 4 H, d,d'-H), 3.43 (AB, J_{AB} = 14.5, $\Delta\nu$ = 28 Hz, 4 H, c,c'-H), 3.77 (s, 2 H, c''-H), 3.79 (s, 2 H, d''-H), 5.60 (d, $^2J_{H,H}$ = 5.8 Hz, 2 H, i-H or j-H), 5.69 (d, $^2J_{H,H}$ = 5.8 Hz, 2 H, i-H or j-H), 6.10 (d, $^4J_{H,H}$ = 0.9 Hz, 2 H, f-H), 6.51 (s, 2 H, a-H), 6.77 (d, $^4J_{H,H}$ = 0.9 Hz, 2 H, f'-H), 6.97 (s, 2 H, OH), 7.02 (s, 2 H, f''-H), 7.19 (s, 1 H, a''-H) ppm (see the Supporting Information for the atom numbering). HRMS: calcd. for $C_{35}H_{36}NaO_6S_6$ 767.07283; found 767.07713.

X-ray Diffraction: Single crystals of **1** were grown by slow evaporation of a CH_2Cl_2 solution. Compound **1** crystallizes in the triclinic system (space group $P\bar{1}$) with two molecules per unit cell ($Z = 2$). Unit cell parameters at $T = 100(2)$ K are $a = 9.0838(11)$, $b = 9.4446(13)$, $c = 17.2029(19)$ Å, $\alpha = 101.302(6)$, $\beta = 99.299(6)$, $\gamma = 98.227(7)^\circ$. A colorless single-crystal specimen of prismatic shape ($0.2 \times 0.2 \times 0.2$ mm³) was selected for the X-ray diffraction experiment at $T = 100(2)$ K. The X-ray source used was graphite-monochromatized Mo- K_α radiation ($\lambda = 0.71073$ Å) from a sealed tube. Data were collected with a Nonius-KappaCCD diffractometer equipped with a nitrogen jet stream low-temperature system (Oxford Cryosystems) and by using the COLLECT software.^[19] Lattice parameters were obtained by a least-squares fit to the optimized setting angles of 6717 collected reflections in the full θ range data collection $1.23 < \theta < 27.98^\circ$. Intensity data were recorded as ϕ and ω scans with κ offsets. Data reduction was performed by using DENZO software^[20] and did not require absorption corrections. The structure was solved by direct methods using the SIR92 pro-

gram.^[21] Refinements were carried out by full-matrix least-squares on F^2 using the SHELXL-97 program^[22] and the complete set of reflections. Anisotropic thermal parameters were used for non-hydrogen atoms. In the crystal structure determination, all hydrogen atoms were located in the Fourier synthesis. They were placed at calculated positions on their carrier atom X(-H) using the riding model with an isotropic thermal factor fixed at $U_{iso}(H) = 1.2U_{eq}(X)$. The structure was converged into the final statistical agreement factors: $R1 = 0.0413$ and 0.0461 for $I > 2\sigma(I)$ and all data, respectively. Further crystal data and structure refinement details are given in Table S1. Figure 2 was drawn using the ORTEP3 for Windows program.^[23]

CCDC-754731 contains the supplementary crystallographic data for this paper. These data can be obtained free of charge from The Cambridge Crystallographic Data Centre via www.ccdc.cam.ac.uk/data_request/cif.

Calculations: All calculations were performed in the gas phase with the Gaussian03 program package^[24] using density functional theory (DFT) with the hybrid exchange-correlation PBE1PBE functional.^[25] The molecular structures of **1–4** were optimized using the 6-311G** basis set for all elements except bromine for which the LANL08d^[26] effective core potential and basis set were used.

Experimental X-ray structures are only known for **1** and **2**, which display collapsed and elongated shapes, respectively. These molecular structures were used as the starting points for the theoretical gas-phase structural optimizations. As shown in Figure S18, the optimized molecular structures are very similar to the experimental ones. To study the preference of these compounds for a given conformation (either elongated or collapsed), hypothetical **1**-elongated and **2**-collapsed forms were created from the experimental structures using appropriate substitutions and then optimized in the gas phase. For compounds **3** and **4**, no crystal of suitable quality for X-ray experiment could be obtained. Thus, initially collapsed and elongated forms were created for both compounds from the experimental structures of **1** and **2** by using appropriate substitutions and then optimized (Figures S21 and S22).

To check that all the calculated structures corresponded to true energy minima and also to compute zero-point energy corrections, frequency calculations were finally performed at the same level of theory on each optimized cage.

Supporting Information (see also the footnote on the first page of this article): $^1H/^{13}C$ NOESY NMR spectra of macrotricyclics **1** and **4** and macrobicyclic **4a**, $^1H/^{13}C$ HSQC and HMBC NMR spectra of macrotricyclics **1** and **4**, ^{13}C NMR spectra of tripod **6** and macrotricyclics **3** and **4**, VT 1H NMR spectra of macrotricyclics **1** and **3**. ESI-HRMS of macrobicyclic **4a** and macrotricyclics **3** and **4**, details of the calculations of the gas-phase structures of macrotricyclics **1**, **2**, **3**, and **4**, and figures showing the calculated structures, table of crystallographic data for macrotricyclic **1**.

Acknowledgments

The Centre National de la Recherche Scientifique (CNRS) and the Conseil Régional de Bourgogne are acknowledged for a doctoral fellowship (A. L.-V.). M.-J. Penouilh is thanked for ESI HRMS measurements. E. Wenger and the “Plateforme de Mesures de Diffraction X” of the CRM2 laboratory are acknowledged for supporting the XRD experiment. The Institut Jean Barriol (Nancy Université) and GENCI-CINES (Grant 2009-X2009085106) are thanked for providing access to computational facilities. We are

grateful to J. Ángyán for fruitful discussions and we thank F. Hoffmann for help with the computational facility.

- [1] C. J. Pedersen, *Angew. Chem. Int. Ed. Engl.* **1988**, *27*, 1021–1027.
- [2] J.-M. Lehn, *Angew. Chem. Int. Ed. Engl.* **1988**, *27*, 89–112.
- [3] D. J. Cram, *Angew. Chem. Int. Ed. Engl.* **1988**, *27*, 1009–1020.
- [4] D. J. Cram, *Angew. Chem. Int. Ed. Engl.* **1986**, *25*, 1039–1057.
- [5] a) C. D. Gutsche, *Calixarenes*, Royal Society of Chemistry, Cambridge, **1989**; b) V. Böhmer, *Angew. Chem. Int. Ed. Engl.* **1995**, *34*, 713–745.
- [6] A. Ikeda, S. Shinkai, *Chem. Rev.* **1997**, *97*, 1713–1734.
- [7] A. Lélías-Vanderperre, J.-C. Chambron, E. Espinosa, P. Terrier, E. Leize-Wagner, *Org. Lett.* **2007**, *9*, 2961–2964.
- [8] K. Araki, H. Hayashida, *Tetrahedron Lett.* **2000**, *41*, 1807–1810.
- [9] A. Lélías-Vanderperre, Ph. D. Thesis, Université de Bourgogne, **2008**.
- [10] a) Y. Rondelez, M.-N. Rager, A. Duprat, O. Reinaud, *J. Am. Chem. Soc.* **2002**, *124*, 1334–1340; b) E. Engeldinger, D. Armspach, D. Matt, *Chem. Rev.* **2003**, *103*, 4147–4173.
- [11] J. Hirsch, S. DeBeer George, E. I. Solomon, B. Hedman, K. O. Hodgson, J. N. Burstyn, *Inorg. Chem.* **2001**, *40*, 2439–2441.
- [12] a) L. Wambach, F. Vögtle, *Tetrahedron Lett.* **1985**, *26*, 1483–1486; b) H. An, J. S. Bradshaw, R. M. Izatt, *Chem. Rev.* **1992**, *92*, 543–572; c) R. Méric, J.-M. Lehn, J.-P. Vigneron, *Bull. Soc. Chim. Fr.* **1994**, *131*, 579–583; d) J. Gross, G. Harder, A. Siepen, J. Harren, F. Vögtle, H. Stephan, K. Gloe, B. Ahlers, K. Cammann, K. Rissanen, *Chem. Eur. J.* **1996**, *2*, 1585–1595.
- [13] D. J. Cram, S. Karbach, H.-E. Kim, C. B. Knobler, E. F. Maverick, J. L. Ericson, R. C. Helgeson, *J. Am. Chem. Soc.* **1988**, *110*, 2229–2237.
- [14] A different synthesis of **9** from **7** was published while this work was in progress and used MOMCl/K₂CO₃ followed by LiAlH₄, see: Q. Wang, Q. Huang, B. Chen, J. Lu, H. Wang, X. She, X. Pan, *Angew. Chem. Int. Ed.* **2006**, *45*, 3651–3653.
- [15] S. P. Hollinshead, J. B. Nichols, J. W. Wilson, *J. Org. Chem.* **1994**, *59*, 6703–6709.
- [16] N. Kumagai, S. Matsunaga, T. Kinoshita, S. Harada, S. Okada, S. Sakamoto, K. Yamaguchi, M. Shibasaki, *J. Am. Chem. Soc.* **2003**, *125*, 2169–2178.
- [17] The shapes of the macrotricycles of this study refer to the polyhedron formed by the centers of the aromatic rings.
- [18] a) W. P. Cochrane, P. L. Pauson, T. S. Sevens, *J. Chem. Soc. C* **1968**, 630–632; b) E. Díez-Barra, J. C. García-Martínez, S. Merino, R. del Rey, J. Rodríguez-López, P. Sánchez-Verdú, J. Tejada, *J. Org. Chem.* **2001**, *66*, 5664–5670.
- [19] B. Nonius, *COLLECT, Data Collection Software*, BV Nonius, Delft, The Netherlands, **1998**.
- [20] DENZO-SCALEPACK: Z. Otwinowski, W. Minor, *Methods in Enzymology*, vol. 276: *Macromolecular Crystallography*, Part A (Eds.: C. W. Carter Jr., R. M. Sweet), Academic Press, **1997**, pp. 307–326.
- [21] SIR92: A. Altomare, G. Casciarano, C. Giacovazzo, A. Guagliardi, *J. Appl. Crystallogr.* **1993**, *26*, 343–350.
- [22] G. M. Sheldrick, *SHELX97 - Programs for Crystal Structure Analysis*, University of Göttingen, Göttingen, **1998**.
- [23] ORTEP3 for Windows: L. J. Farrugia, *J. Appl. Crystallogr.* **1997**, *30*, 565.
- [24] M. J. Frisch, G. W. Trucks, H. B. Schlegel, G. E. Scuseria, M. A. Robb, J. R. Cheeseman, J. A. Montgomery Jr., T. Vreven, K. N. Kudin, J. C. Burant, J. M. Millam, S. S. Iyengar, J. Tomasi, V. Barone, B. Mennucci, M. Cossi, G. Scalmani, N. Rega, G. A. Petersson, H. Nakatsuji, M. Hada, M. Ehara, K. Toyota, R. Fukuda, J. Hasegawa, M. Ishida, T. Nakajima, Y. Honda, O. Kitao, H. Nakai, M. Klene, X. Li, J. E. Knox, H. P. Hratchian, J. B. Cross, V. Bakken, C. Adamo, J. Jaramillo, R. Gomperts, R. E. Stratmann, O. Yazyev, A. J. Austin, R. Cammi, C. Pomelli, J. W. Ochterski, P. Y. Ayala, K. Morokuma, G. A. Voth, P. Salvador, J. J. Dannenberg, V. G. Zakrzewski, S. Dapprich, A. D. Daniels, M. C. Strain, O. Farkas, D. K. Malick, A. D. Rabuck, K. Raghavachari, J. B. Foresman, J. V. Ortiz, Q. Cui, A. G. Baboul, S. Clifford, J. Cioslowski, B. B. Stefanov, G. Liu, A. Liashenko, P. Piskorz, I. Komaromi, R. L. Martin, D. J. Fox, T. Keith, M. A. Al-Laham, C. Y. Peng, A. Nanayakkara, M. Challacombe, P. M. W. Gill, B. Johnson, W. Chen, M. W. Wong, C. Gonzalez, J. A. Pople, *Gaussian 03*, rev. B.05, Gaussian, Inc., Wallingford, CT, **2004**.
- [25] C. Adamo, V. Barone, *J. Chem. Phys.* **1999**, *110*, 6158–6169.
- [26] L. E. Roy, P. J. Hay, R. L. Martin, *J. Chem. Theory Comput.* **2008**, *4*, 1029–1031.

Received: December 2, 2009
Published Online: April 7, 2010